Macromolecular Research, Vol. 16, No. 4, pp 337-344 (2008)

Synthesis and Characterization of Spirobifluorene-Based Polymers for Organic Light-Emitting Diode Applications

Md. Anwarul Karim and Young-Rae Cho

Department of Materials Science and Engineering, Pusan National University, Busan 609-735, Korea

Jin Su Park, Kyung-Jin Yoon, Seung Joon Lee, and Sung-Ho Jin*

Department of Chemistry Education and Interdisciplinary Program of Advanced Information and Display Materials, Pusan National University, Busan 609-735, Korea

Gi-Dong Lee*

Department of Electronics Engineering, Dong-A University, Busan 604-714, Korea

Yeong-Soon Gal

Polymer Chemistry Lab., Kyungil University, Hayang 712-701, Korea

Received October 31, 2007; Revissed February 5, 2008; Accepted February 9, 2008

Abstract: The following series of blue EL polymers was synthesized using the Suzuki polymerization method: poly(3′,6′-bis(3,7-dimethyloctyloxy)-9,9′-spirobifluorene-2,7-diyl) poly[$(OC_{10})_2$-spirobifluorene], poly{3′,6′-bis(3,7-dimethyloctyloxy)-9,9′-2,7-diyl-*co*-4-(3,7-dimethyloctyloxy) phenyl-diphenylamine-4′,4′-diyl} poly[$(OC_{10})_2$-spirobifluorene-TPA] (5:1, 9:1) and poly{3′,6′-bis(3,7-dimethyloctyloxy)-9,9′-spirobifluorene-2,7-diyl-*co*-4-(6-((3-methyloxetan-3-yl)methoxy)hexyloxyphenyl-bisphenylamine-4′,4′-diyl) poly[$(OC_{10})_2$-spirobifluorene-TPA-oxetane]. The weight average molecular weight (Mw) and polydispersity of the resulting polymers ranged from 1.6×10^4-1.5×10^5 and 1.77-2.31, respectively. The resulting polymers were completely soluble in common organic solvents and were easily spin-coated onto an indium tin oxide (ITO) substrate. The polymers exhibited strong blue emission peaking at 450 nm. The maximum brightness and luminance efficiency were 9,960 cd/m^2 and 1.2 cd/A, respectively.

Keywords: PLED, interlayer, poly(spirobifluorene), oxetane.

Introduction

There has been remarkable improvement in the device performance of polymer light-emitting diodes (PLEDs) since the first electroluminescence (EL) prototype was reported by the Cambridge group in 1990.[1] Among π-conjugated polymers, poly(*p*-phenylenevinylenes) (PPVs),[2,3] polythiophenes (PThs),[4] poly(9,9-dialkylfluorenes) (PFs)[5,6] and their derivatives have been widely used as the most powerful candidates for application to PLEDs. However, new thermally stable emissive and charge transport polymers are needed to improve their device performance and durability. PFs containing two planarized benzene rings per monomeric unit have many advantages such as chemical and thermal stability, high photoluminescence (PL) quantum efficiency, and easy tuning ability through copolymerization with various comonomers. The most serious drawbacks of PFs are a tendency to form chain aggregation or keto-defect for longer wavelength emission upon heating or the application of a current during device fabrication or operation.[7] In order to solve these problems, fluorene substituents were incorporated into the carbon 9-position of the fluorene main chain to achieve a spirobifluorene-segment. In the spiro-segment, the bifluorenes were arranged orthogonally, and the resulting polymer chains were twisted at an angle of 90° at each spiro-center.[8] This structural feature is expected to reduce the likelihood of interchain interactions and prevent close packing of the polymer chains. Triphenylamine (TPA)-based EL copolymers made the hole injection easier from PEDOT:PSS to the emitting layer by lowering the HOMO level of the emitting layer to less than that of the homopolymer. Our research efforts on PLEDs have shown that the insertion of a thin π-conjugated polymer interlayer between

*Corresponding Authors. E-mails: shjin@pusan.ac.kr, gdlee@donga.ac.kr

PEDOT:PSS and an emissive layer to prevent exciton quenching at the PEDOT:PSS interface, which makes easily hole injection, significantly improves the device efficiency of PLEDs.[9-11]

In this paper, the following spirobifluorene-based homopolymers were synthesized and characterized for the realization of blue EL polymers: poly(3′,6′-bis(3,7-dimethyloctyloxy)-9,9′-spirobifluorene-2,7-diyl), poly[$(OC_{10})_2$-spirobifluorene], and its copolymers, poly{3′,6′-bis(3,7-dimethyloctyloxy)-9,9′-spirobifluorene-2,7-diyl-*co*-4-(3,7-dimethyloctyloxy)phenyl-diphenylamine-4′,4′-diyl}, poly[$(OC_{10})_2$-spirobifluorene-TPA] (5:1, 9:1) with different ratios of the TPA derivative. In addition, the polymer interlayer, poly{3′,6′-bis(3,7-dimethyloctyloxy)-9,9′-spirobifluorene-2,7-diyl-*co*-4-(6-((3-methyloxetan-3-yl)methoxy)hexyloxyphenyl-bisphenylamine-4′,4′-diyl)} poly[$(OC_{10})_2$-spirobifluorene-TPA-oxetane], which has a crosslinking moiety on the polymer backbone as a side chain, was synthesized to improve the device performance. The resulting EL polymers were synthesized using the Suzuki polymerization method, and their EL properties were characterized.

Experimental

Materials. Fluorene, 3,3′-dimethoxybiphenyl, *tert*-butyllithium in pentane (1.7 M), *N*-bromosuccinimide, glacial acetic acid, 3,7-dimethyloctanol, methyl sulfide, bromine, diphenylamine, 4-iodophenol, tetrabutylammonium tribromide (98%), 4-iodophenol, 1,6-dibromohexane, 3-methyl-3-oxetane methanol (98%), palladium (II) acetate, copper (I) chloride (97%), 1,10-phenanthroline, tricyclohexylphosphine, tetraethylammonium hydroxide (20 wt% solution in water), 9-bromoanthracene, and 2-isopropoxy-4,4,5,5-tetramethyl-1,3,2-dioxaborolane (98%) were purchased from Aldrich Chemical Co and TCI organic chemicals. These chemicals were used without further purification unless otherwise noted. Solvents were dried and purified by fractional distillation over sodium/benzophenone and handled in moisture-free atmosphere. Column chromatography was performed using silica gel (Merck, 250-430 mesh). The synthesis of Monomer-I,-II,-III, poly[$(OC_{10})_2$-spirobifluorene] and poly[$(OC_{10})_2$-spirobifluorene-TPA] with various feed ratios were prepared according to our previous report.[12]

Instruments, Measurements, and Device Fabrication. ^{1}H-NMR spectra were recorded using a Bruker AM-300 spectrometer and chemical shift were recorded in ppm unit. The UV-vis spectrum was recorded on a Shimadzu UV-3100 spectrophotometer. Molecular weight and polydispersity of polymers were determined by gel permeation chromatography (GPC) analysis relative to polystyrene calibration (Agilent 1100 series GPC, PL gel 5 μm MIXED-C, refractive index detector) in THF solution. Thermal analyses were carried out on a Mettler Toledo TGA/SDTA 851, DSC 822 analyzer under an N_2 atmosphere at a heating rate of 10 °C/min. Optical thin films of the polymers were obtained by spin-coating based on toluene or chlorobenzene solution. All polymer solutions were filtered with 0.45 μm PP syringe filters (Whatman) prior to spin-coating. PL studies were carried out using a F-4500 Fluorescence spectrophotometer (HITACHI). Cyclic voltammetry (CV) was carried out with a Bioanalytical Systems CV-50W voltammetric analyzer at a potential scan rate of 50-100 mV/s in 0.1 M solution of tetrabutylammonium tetrafluoroborate (Bu_4NBF_4) in anhydrous acetonitrile. Each polymer film was coated on a Pt disc electrode (0.2 cm^2) by dipping the electrode into the polymer solution. A platinum wire was used as the counter electrode, and an $Ag/AgNO_3$ electrode was used as the reference electrode. All of the electrochemical experiments were performed in a glove box under an Ar atmosphere at room temperature. For the insertion of polymer interlayer, poly(RO_2-spiro-TPA-oxetane) solutions (2 wt%) in anhydrous toluene were first prepared and then blended with photoacid generator (PAG; triphenylsulfonium triflate, TPSOTf) (1 wt%) and spin-coated directly on top of the PEDOT:PSS layer with 1,500 rpm for 40 sec.

The film was exposed to 365 nm UV-light of 30 mJ/cm^2 intensity for 30 sec and annealed at 180 °C for 10 min.[13] Afterwards, the film was rinsed by chlorobenzene several times and finally annealed at 180 °C for 2-3 min. Solid-state emission measurements was achieved using film supported on a quartz substrate and mounted with front-face excitation at an angle of < 45°. The polymer film was excited with several portions of visible light from a Xenon lamp. To measure EL, PLED was constructed as follows: The glass substrate coated with a transparent ITO electrode was thoroughly cleaned by successive ultrasonic treatments in acetone, isopropyl alcohol, and distilled water then dried with N_2 gas and heated for further drying. The polymer film was prepared by spin casting a polymer in chlorobenzene or toluene solution (0.5-1.5 wt%). Uniform and pinhole-free films with a thickness around 80-110 nm were easily obtained from the resulting polymer solution. LiF, Ca, and Al metal were deposited on the top of polymer film through a mask by vacuum evaporation at pressures below 1×10^{-6} Torr, yielding active areas of 4 mm^2. For the measurements of device characteristics, current density-voltage-luminescence (J-V-L) changes were measured using a current/voltage source (Keithly 236) and an optical power meter (CS-1000, LS-100). All processes and measurements mentioned above were carried out in the open air at room temperature.

Synthesis of 1-(6-bromohexyloxy)-4-iodobenzene. A mixture of 4-iodophenol (4.5 g, 25 mmol), potassium carbonate (6.3 g, 50 mmol) was added to dried acetonitrile (100 mL) and stirred for 2-3 h at 110 °C. 1,6-Dibromohexane was dropwised (6.3 mL, 50 mmol) to the mixture. The mixture was refluxed for 18 h at 110 °C, extracted with ethyl acetate, and dried with anhydrous $MgSO_4$. Purification by column chromatography (hexane:methylene chloride=5:1)

to give a white product, 1-(6-bromohexyloxy)-4-iodobenzene (5.25 g, yield : 67%).

^{1}H-NMR ($CDCl_3$): δ (ppm) 7.6-7.48(d, *J*=8 Hz 2H), 6.72-6.60 (d, *J*=8 Hz 2H), 3.94-3.90 (t, *J*=6 Hz 2H), 3.45-3.41 (t, *J*=6 Hz, 2H), 1.92-1.77 (m, 4H), 1.54-1.49 (m, 4H).

Synthesis of 3-(6-(4-iodophenoxy)hexyloxymethyl)-3-methyloxetane. To a solution of 50% aqueous NaOH (18.4 g), hexane (25 mL) and tetrabutylammonium bromide (0.22 g), 1-(6-bromohexyloxy)-4-iodobenzene (5.25 g 13.7 mmol) and 3-methyl-3-oxetane methanol (1.43 g, 13.7 mmol) were added. The mixture was refluxed for 2 h. After cooling down to room temperature, it was diluted with water (100 mL) and extracted with diethyl ether. The combined organic layer was dried with anhydrous $MgSO_4$ and the solvent was removed in vacuum. Purification by column chromatography (hexane:ethyl acetate=9:1) gave a colorless liquid product, 3-(6-(4-iodophenoxy)hexyloxymethyl)-3-methyloxetane (3.3 g yield : 60%).

^{1}H-NMR ($CDCl_3$): δ (ppm) 7.6-7.48(d, *J*=8 Hz 2H), 6.72-6.60 (d, *J*=8 Hz 2H), 4.50-4.48 (d, *J*=5 Hz 2H), 4.35-4.33 (d, *J*=5 Hz, 2H), 3.92-3.87(t, *J*=6 Hz, 2H), 3.48-3.43 (m, 4H) 1.81-1.27 (m, 11H).

Synthesis of bis(4-bromophenyl)amine. Tetrabutylammonium tribromide (11.4 g, 11.8 mmol) was added to the solution of diphenylamine (2 g, 11.8 mmol) in chloroform (15 mL) at room temperature. The reaction time was about 20 min with TLC check until the starting material spot was removed. The resulting solution was washed with aqueous sodium thiosulfate, then neutralized with water to the pH 7, then extracted with diethyl ether and water and dried with anhydrous $MgSO_4$. Purification by column chromatography (hexane:ethyl acetate=8:1) to give a bright yellow product, bis(4-bromophenyl)amine (2.5 g, yield : 64%).

^{1}H-NMR (DMSO): δ (ppm) 8.46 (s, 1H), 7.34-7.37 (d, *J*= 9 Hz 2H), 6.99-6.96 (d, *J*=8 Hz 2H).

Synthesis of 4-(6-(3-methyloxetan-3-yl)methoxyhexyloxy)phenyl-bis(4′-bromophenyl)amine (Monomer-IV). A mixture of bis(4-bromophenyl)amine (2 g, 6.1 mmol), 3-(6-(4-iodophenoxy)hexyloxymethyl)- 3-methyloxetane (2.05 g, 5.1 mmol), KOH (2.3 g, 40 mmol), cuprous chloride (0.04 g), and 1,10-phenanthroline (0.04 g) in toluene (10 mL) was refluxed at 125 °C for 20 h. The water was removed with a fixed Dean-Stark trap. After completion of the reaction, the mixture was cooled to room temperature and poured into water (300 mL) and then extracted with chloroform. The organic layer was washed with a dilute solution of ammonium hydroxide and water successively, dried with anhydrous $MgSO_4$ and the solvent was removed in vacuum.. Purification by column chromatography (hexane: ethyl acetate=7:2) give a yellow liquid product, 4-(6-(3-methyloxetan-3-yl)methoxyhexyloxy)phenyl-bis (4′-bromophenyl)amine (2.5 g yield : 82%).

^{1}H-NMR ($CDCl_3$): δ (ppm) 7.30-7.25 (m, 4H), 7.02-6.6.99 (d, *J*=8 Hz 2H), 6.89-6.80 (m, 6H) 4.50-4.48 (d, *J*=5 Hz 2H), 4.35-4.33 (d, *J*=5 Hz, 2H), 3.92-3.87 (t, *J*=6 Hz, 2H), 3.48-3.43 (m, 4H) 1.81-1.27 (m, 11H).

Synthesis of Poly{3′,6′-bis(3,7-dimethyloctyloxy)-9,9′-spirobifluorene-2,7-diyl-*co*-4-(6-((3-methyloxetan-3-yl)-methoxy)hexyloxyphenyl-bisphenylamine-4′,4′-diyl), Poly[$(OC_{10})_2$-Spirobifluorene-TPA-Oxetane]. In a dried 3-neck round bottom flask, 2,7-bis(4,4,5,5-tetramethyl-1,3,2-dioxaborolane-2-yl)-3′,6′-bis(3,7-dimethyloctyloxy)-9,9′ spirobifluorene (0.25 g, 0.28 mmol), 4-(6-(3-methyloxetan-3-yl)methoxyhexyloxy)phenyl-bis(4′-bromophenyl)-amine (0.168 g, 0.28 mmol), palladium(II) acetate (1.6 mg, 2.5 mol%) and tricyclohexylphosphine (6.4 mg, 8 mol%) were added under N_2 atmosphere. Dried toluene (3 mL) was added and the mixture was stirred at 90 °C for 5 min. 20% w/w tetraethylammonium hydroxide aqueous solution (1.5 mL) was added. The mixture was stirred for a further 36 h. To the mixture anthracenylboronic acid (0.05 g) was added and after stirring for 2 h, then bromoanthracene (0.12 g) was added. After stirring for a further 4 h, the polymerization solution was poured into 600 mL of methanol and the crude polymer was successively Soxhlet extracted with methanol, isopropyl alcohol, and hexane to remove the unreacted monomers, impurities and oligomers. The polymerization solution was filtered through silica plug, and the resulting polymer was redissolved in chloroform and reprecipitated in stirring methanol (300 mL). The precipitated product was filtered and then dried in vacuo to give the dark brown solid product (0.12 g, yield: 41%).

^{1}H-NMR ($CDCl_3$): δ (ppm) 6.6-7.1 (br, 13H, aromatic protons), 7.3 (br, 3H, aromatic proton), 7.5-7.9 (br, 2H aromatic proton), 4.5 (2H), 4.35 (2H), 4.1-4.0 (br, 4H), 3.9 (2H), 3.5 (4H), 1.9-0.7 (br, 65H).

Results and Discussion

The spirobifluorene segment was introduced into the polymer backbone by synthesizing the monomer-I, -II, and -III according to the reported procedures.[12] Spirobifluorene-based EL polymers, poly[$(OC_{10})_2$-spirobifluorene], poly [$(OC_{10})_2$-spirobifluorene-TPA] (5:1, 9:1) and polymer interlayer, poly[$(OC_{10})_2$-spirobifluorene-TPA-oxetane], were synthesized using Suzuki polymerization method, as shown in Scheme I.[14] Polymerization was carried out using palladium(II) acetate, tricyclohexylphosphine, an aqueous solution of tetraethylammonium hydroxide (20% w/w) in dried toluene under an N_2 atmosphere for 36 h. During polymerization, a strong fluorescent light was observed without any precipitation. The key factor for obtaining the high molecular weight polymers is the use of palladium(II) acetate instead of tetrakis(triphenylphophine)palladium(0). The reaction using palladium(II) was more easily controlled in air due to the better stabilization of palladium(II) in air than palladium(0). In order to improve the color purity and PLED performance, the resulting EL polymers were further puri-

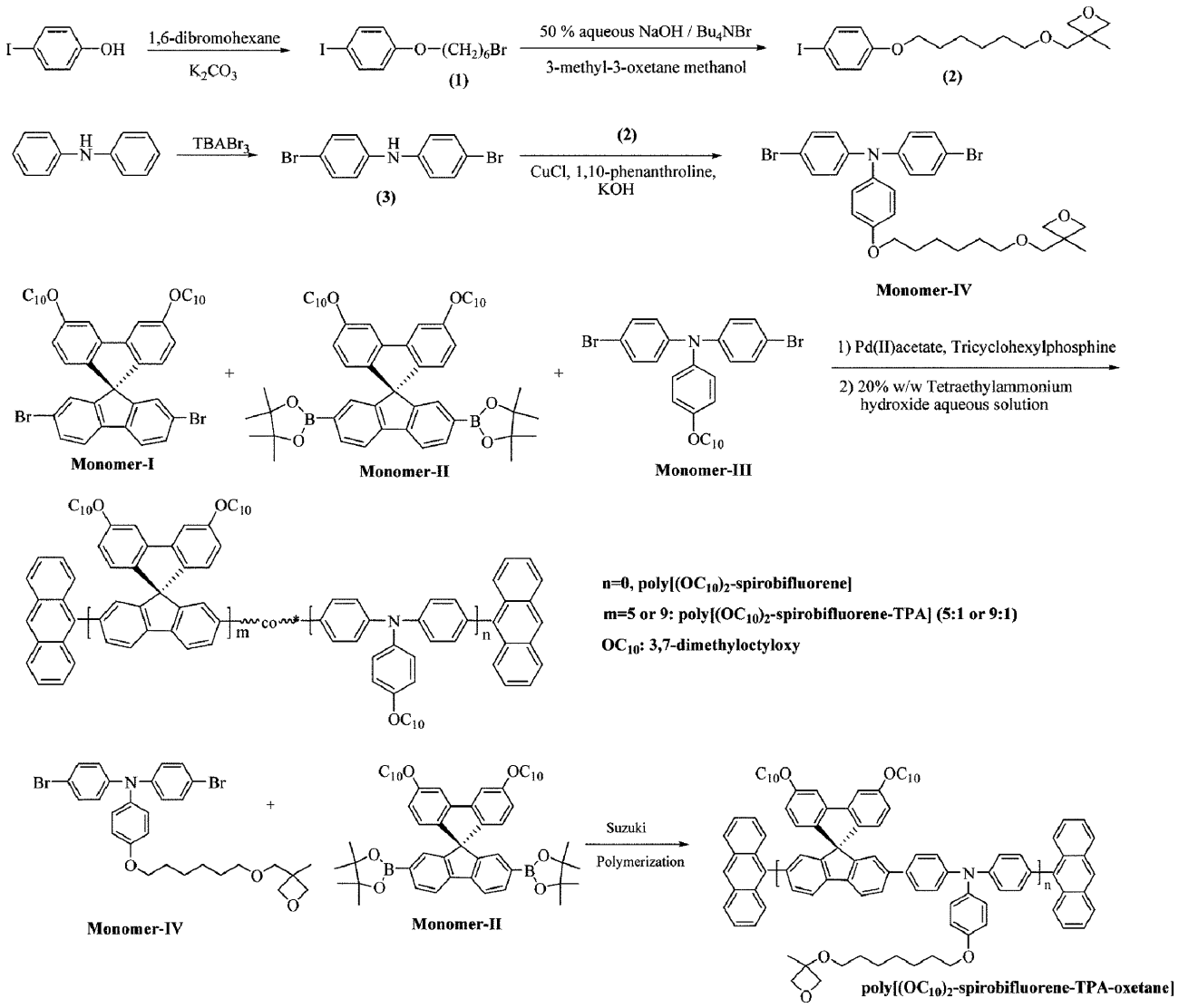

Scheme I

fied by multiple Soxhlet extraction with different solvents including methanol, acetone, and finally chloroform to remove the unreacted monomers, oligomers, and polymers with a medium molecular weight. From these processes, a highly purified and narrow polydispersity of the polymers were obtained. The resulting polymers were completely soluble in various organic solvents such as chloroform, chlorobenzene, toluene, and xylene, etc. The molecular structures of the monomers and the polymers were identified by ^{1}H-NMR and elemental analysis. Figure 1 shows the ^{1}H-NMR spectra of poly[$(OC_{10})_2$-spirobifluorene], poly[$(OC_{10})_2$-spirobifluorene-TPA] (9:1), and poly[$(OC_{10})_2$-spirobifluorene-TPA] (5:1) in $CDCl_3$. The ^{1}H-NMR spectra of the polymers are not sufficient to characterize the composition ratio of the copolymers. This is because almost all proton peaks were located in the aromatic range and the methoxy or alkylation proton peaks were in a similar region.

Table I summarizes the polymerization results, molecular weights, polydispersity, and thermal characteristics of the polymers. The weight-average molecular weight (M_w) and polydispersity of the polymers ranged from 1.6×10^4-2.7×10^5 and 1.77-2.31, respectively. The thermal behaviors of the polymers were examined by DSC and TGA. The glass transition temperatures of the polymers ranged from 146 to 293 °C. TGA thermograms were measured at the temperature of 5% weight loss for all polymers and showed the stable up to 369-415 °C. A higher thermal stability was obtained by introducing a spirobifluorene segment on the polymer backbone. The thermal stability of the emitting layer and polymer interlayer is one of the most critical requirements for OLEDs particularly for the blue emitting layer because it requires a higher turn on voltage than the other color emitting polymers. The polymers showing high thermal stability were resistant to deformation and device degradation caused

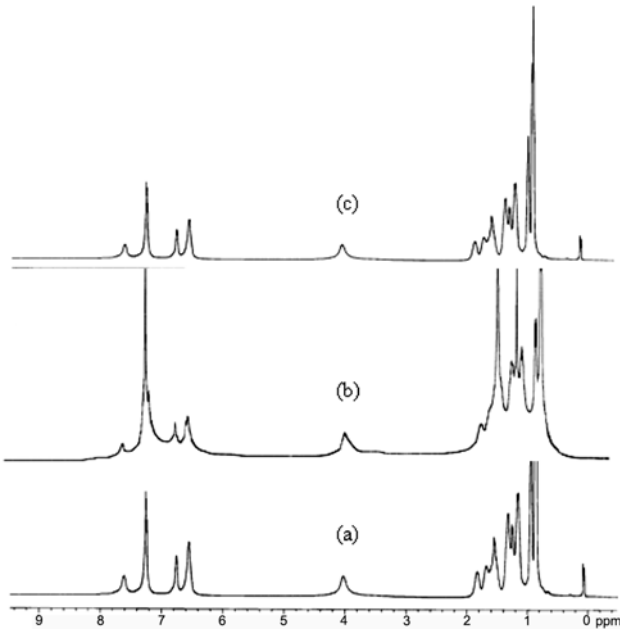

Figure 1. ^{1}H-NMR spectra of (a) poly[$(OC_{10})_2$-spirobifluorene], (b) poly[$(OC_{10})_2$-spirobifluorene-TPA] (5:1), and (c) poly[$(OC_{10})_2$-spirobifluorene-TPA] (9:1).

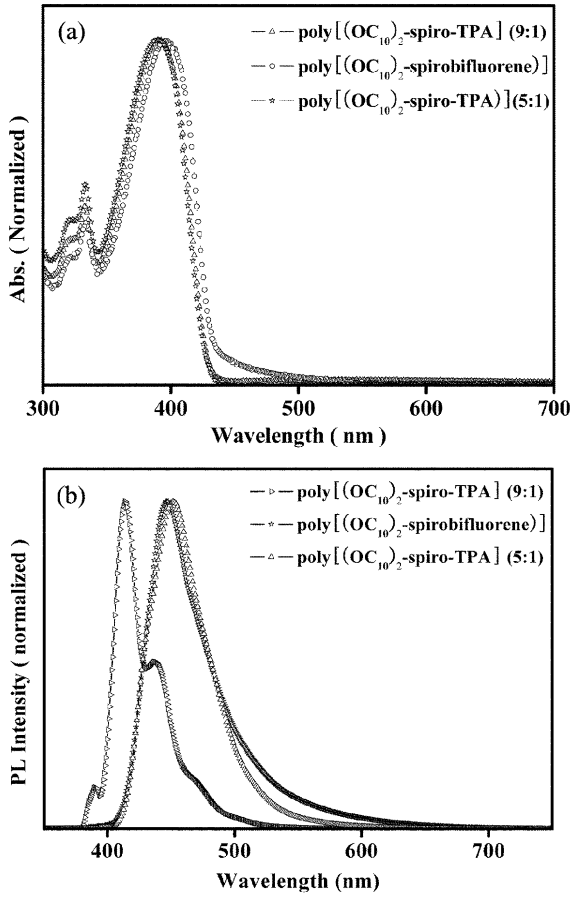

Figure 2. UV-visible and Photoluminescence (PL) spectra of EL polymers in film state.

by current-induced heating during the operation of OLEDs.

Figure 2 shows the UV-visible absorption and PL emission spectra of the polymers in thin film state. The maximum absorption peak of poly[$(OC_{10})_2$-spirobifluorene] and poly[$(OC_{10})_2$-spirobifluorene-TPA] (5:1, 9:1) in the film state were located in the range of 390 and 395 nm, which is due to the π-π* transition of the π-conjugated polymer backbone. The emission peak of poly[$(OC_{10})_2$-spirobifluorene] and poly[$(OC_{10})_2$-spirobifluorene-TPA] (9:1, 5:1) in the film state ranged from 428-452 nm.

In order to provide information on charge injection and the device performance, it is important to calculate the energy band diagram from electrochemical measurements using CV for the HOMO binding energy with ferrocene as the standard, and the band gap from the optical absorption spectrum. The HOMO and LUMO energy levels were estimated from the onset oxidation data and optical band edge. Figure 3 shows the hypothesized energy diagrams of the ITO/PEDOT/polymer/cathode device fabricated in this study. The HOMO and band gap of poly[$(OC_{10})_2$-spirobifluorene] were approximately 5.51 and 2.89 eV, respectively. This shows that PEDOT:PSS has a high energy barrier, which makes it difficult for a hole to be injected from the hole injection layer to the emitting layer. However, when the TPA repeating unit was introduced into the polymer backbone, the HOMO levels of poly[$(OC_{10})_2$-spirobifluorene-TPA] (5:1, 9:1) were increased from 5.51 eV to 5.35 and 5.24 eV. The decreasing energy barrier makes hole injection

Table I. Polymerization Results and Thermal Properties of Poly[$(OC_{10})_2$-Spirobifluorene], Poly[$(OC_{10})_2$-Spirobifluorene-TPA] and Poly[$(OC_{10})_2$-Spirobifluorene-TPA-Oxetane]

Polymer	Yield (%)	$Mw^a \times 10^4$	PDI^a	DSC/°C	TGA^b/°C
Poly[$(OC_{10})_2$-spirobifluorene]	60	1.6	1.77	293	415
Poly[$(OC_{10})_2$-spirobifluorene-TPA] (5:1)^c	43	7.6	1.91	154	392
Poly[$(OC_{10})_2$-spirobifluorene-TPA] (9:1)^c	53	15	2.31	155	415
Poly[$(OC_{10})_2$-spirobifluorene-TPA-oxetane]	41	27	2.10	146	369

^{a}*Mw* and PDI of the polymers were determined by GPC using polystyrene standards. ^{b}TGA was measured at temperature of 5% weight loss for the polymers. ^{c}Mole ratio of spirobifluorene and TPA segments.

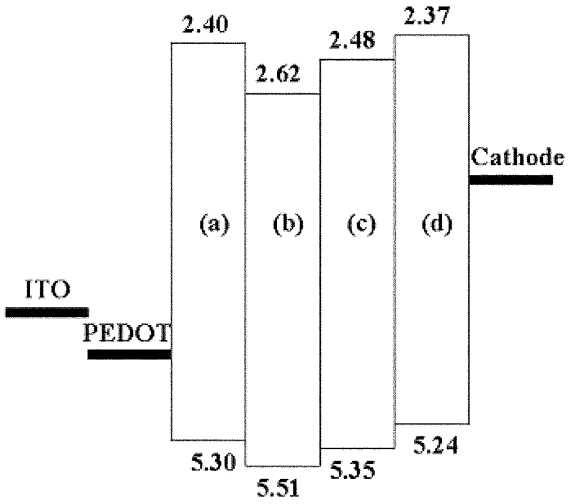

Figure 3. Hypothesized energy diagram of ITO/PEDOT/polymer/cathode devices, poly[$(OC_{10})_2$-spirobifluorene-TPA-oxetane] (a), poly[$(OC_{10})_2$-spirobifluorene] (b), poly[$(OC_{10})_2$-spirobifluorene-TPA] (5:1) (c), and poly[$(OC_{10})_2$-spirobifluorene-TPA] (9:1) (d).

easier than poly[$(OC_{10})_2$-spirobifluorene], which will improve the PLED performance.

PLEDs were fabricated with a configuration of ITO/PEDOT/polymer/cathode to examine the EL properties of the polymers. The cathode was composed of LiF (1 nm)/Al (200 nm) (device 1) or LiF (1 nm)/Ca (20 nm)/Al (200 nm) (device 2). The performance of device 2 was better than that of device 1 (Table II). The devices made using an Al cathode did not show good performance. The poor performance of device 1 was caused by poor electron injection due to the high energy barrier between the LUMO level of the emitting layer and the metal work function. However, the device performance was increased dramatically when Ca was used as the cathode. This was attributed to the lower energy barrier between the LUMO level of the emitting layer and the metal work function, resulting in easy electron injection compared with the Al cathode. The HOMO level of a conducting polymer is closely related to the charge injection and transporting properties of the conjugated polymers. The HOMO level can be controlled by changing the mole ratio of the TPA unit in copolymers from 5.51 eV of poly[$(OC_{10})_2$-spirobifluorene] to 5.24 eV of poly[$(OC_{10})_2$-spirobifluorene-TPA] (9:1). The poly[$(OC_{10})_2$-spirobifluorene-TPA] (9:1) showed well balanced charge injection with the Ca cathode due to the well matched HOMO level for easy hole injection. Moreover, TPA derivatives show good hole transporting properties. Poly[$(OC_{10})_2$-spirobifluorene-TPA] (9:1) showed the best performance among poly[$(OC_{10})_2$-spirobifluorene] and poly[$(OC_{10})_2$-spirobifluorene-TPA] (5:1). Figure 4 shows the current density-voltage-luminescence (J-V-L) curves and luminous efficiencies for device 2. The turn-on voltages of poly[$(OC_{10})_2$-spirobifluorene] and poly[$(OC_{10})_2$-spirobifluorene-TPA] (5:1, 9:1) in device 2 was approximately 5, 5, and 4.5 V, respectively. The turn on voltages were also decreased due to the increased HOMO level of poly[$(OC_{10})_2$-spirobifluorene-TPA] (5:1, 9:1). The maximum luminescences (L_{max}) of poly[$(OC_{10})_2$-spirobifluorene] and poly[$(OC_{10})_2$-spirobifluorene-TPA] (9:1, 5:1) in device 2 were 311 cd/m^2 at 11 V, 9,960 cd/m^2 at 14V, and 518 cd/m^2 at 14V, respectively. And also, the maximum luminance efficiency of poly[$(OC_{10})_2$-spirobifluorene] and poly[$(OC_{10})_2$-spirobifluorene-TPA] (9:1, 5:1) in device 2 were observed as 0.062 cd/A at 11 V, 1.2 cd/A at 13 V, and 0.05 cd/A at 14 V, respectively. Normally, the EL spectrum of PFs shows an additional broad band between 500 and 600 nm due to aggregation or a keto-defect. However, poly[$(OC_{10})_2$-spirobifluorene-TPA] (5:1, 9:1) did not show any long range emission in the EL spectrum. The CIE chromaticity of poly[$(OC_{10})_2$-spirobifluorene-TPA] (9:1) was (0.16, 0.16), which is in the pure blue region.

PLEDs were fabricated with a configuration of ITO/PEDOT/interlayer/emitting layer/LiF/Ca/Al structures using poly[$(OC_{10})_2$-spirobifluorene] as an emitting layer in order to examine the effect of the polymer interlayer on the performance of PLED and the EL performance are summarized in Table III. The reference device structure for the comparison was ITO/PEDOT/polymer/LiF/Ca/Al. In this case, poly[$(OC_{10})_2$-spirobifluorene] was used as the emitting layer instead of poly[$(OC_{10})_2$-spirobifluorene-TPA] (5:1, 9:1) because poly[$(OC_{10})_2$-spirobifluorene] can directly demonstrate the effect from the polymer interlayer. A crosslinking method was used to introduce a polymer interlayer between

Table II. PLED Performance of Poly[$(OC_{10})_2$-Spirobifluorene] and Poly[$(OC_{10})_2$-Spirobifluorene-TPA]

Polymer	Cathode	Turn-On (V)	L_{max}[a], cd/m^2 (V)	LE_{max}[b], cd/A
Poly[$(OC_{10})_2$-spirobifluorene]	LiF/Al	6.0	66 (11 V)	0.045 (8 V)
	LiF/Ca/Al	5.0	311 (11 V)	0.06 (11 V)
Poly[$(OC_{10})_2$-spirobifluorene-TPA] (5:1)	LiF/Al	6.0	20 (14 V)	0.005 (11 V)
	LiF/Ca/Al	5.0	518 (14 V)	0.05 (14 V)
Poly[$(OC_{10})_2$-spirobifluorene-TPA] (9:1)	LiF/Al	6.0	264 (8 V)	0.272 (8 V)
	LiF/Ca/Al	4.5	9960 (8 V)	1.20 (13 V)

[a]Maximum luminescence. [b]Maximum luminance efficiency.

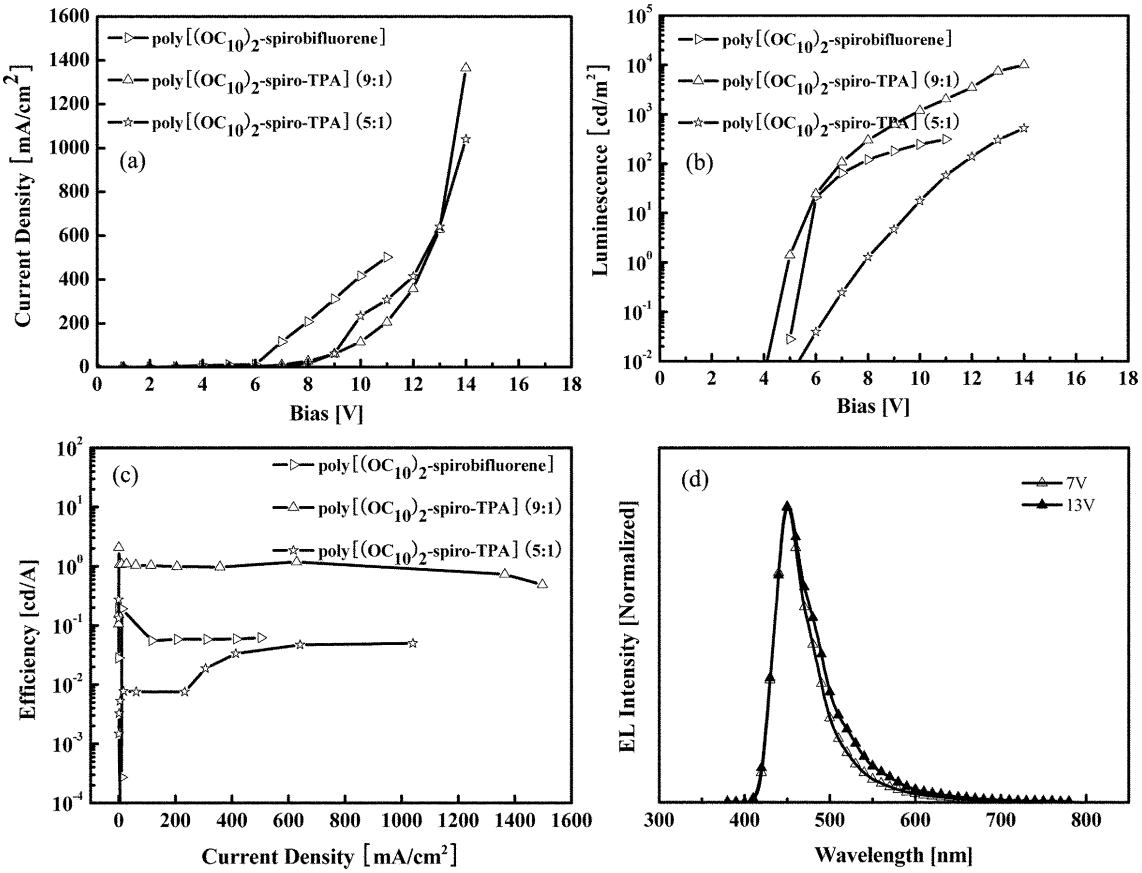

Figure 4. Current density-voltage-luminescence (J-V-L) characteristics and efficiencies of EL polymers (ITO/PEDOT:PSS (30 nm)/ polymer/LiF (1 nm)/Ca (20 nm)/Al (200 nm) and EL spectra of poly[$(OC_{10})_2$-spirobifluorene-TPA] (9:1).

Table III. PLED Performance of Poly[$(OC_{10})_2$-Spirobifluorene] Containing Polymer Interlayer Based on Poly[$(OC_{10})_2$-Spirobifluorene-TPA-Oxetane]

Polymer	PEDOT:PSS	Poly[$(OC_{10})_2$-spirobifluorene-TPA-oxetane]	Turn-On (V)	L_{max}, cd/m^2 (V)	LE_{max}, cd/A
Poly[$(OC_{10})_2$-spirobifluorene]	with	without	5.0	331 (11 V)	0.062 (11 V)
Poly[$(OC_{10})_2$-spirobifluorene]	with	with	7.0	739 (15 V)	0.131 (17 V)
Poly[$(OC_{10})_2$-spirobifluorene]	without	with	7.0	273 (16 V)	0.043 (16 V)

the PEDOT:PSS layer and emitting layer in order to make it more resistant to the organic solvent. The polymer interlayer, poly($(OC_{10})_2$-spiro-TPA-oxetane), showed reasonable HOMO levels for hole injection from PEDOT:PSS. The LUMO level of poly($(OC_{10})_2$-spiro-TPA-oxetane) was 2.40 eV. The high LUMO level of poly($(OC_{10})_2$-spiro-TPA-oxetane) was attributed to the block of radiative excitons from direct quenching by PEDOT:PSS. This property also helps improve the device efficiency with better hole injection and hole transport.

The morphology of the crosslinked interlayer was not so smooth (r.m.s roughness ~5.4 nm), which makes charge injection difficult. Despite these disadvantages, the device efficiency was also increased when the polymer interlayer was introduced. The HOMO and LUMO levels of poly($(OC_{10})_2$-spiro-TPA-oxetane) were 5.3 eV, which contribute to the easily injection of holes from the PEDOT:PSS layer to the emitting layer. Introducing a polymer interlayer resulted in an increase in the maximum brightness and luminance efficiency from 331 cd/m^2 and 0.062 cd/A to 739 cd/m^2 and 0.131 cd/A, respectively.

Conclusions

A new series of blue EL polymers based on poly[$(OC_{10})_2$-spirobifluorene], poly[$(OC_{10})_2$-spirobifluorene-TPA] (5:1, 9:1), and polymer interlayer, poly[$(OC_{10})_2$-spirobifluorene-TPA-oxetane] were synthesized and characterized. The resulting polymers were highly soluble in common organic solvents,

allowing them to be easily spin-coated onto glass substrates with high quality optical thin films. PLEDs were fabricated in ITO/PEDOT/light-emitting polymer/cathode configurations using either a bilayer of LiF/Al or a triple layer of the LiF/Ca/Al cathode structure. It was found that the performance of the PLEDs with the LiF/Ca/Al layer cathodes was higher than with the LiF/Al layer cathodes. The maximum brightness and luminance efficiency of these EL polymers were 9,960 cd/m^2 and 1.2 cd/A, respectively.

Acknowledgment. This research was supported by the Korea Science and Engineering Foundation (KOSEF) grant funded by the Korea government (MOST) (No. M10600000157-06J0000-15710 and the University IT Research Center (ITRC) Project of the Ministry of Information and Communication. We also thank the Korean Ministry of Education (BK 21 Program) for graduate studentships.

References

(1) J. H. Burroughes, D. D. C. Bradley, A. R. Brown, R. N. Marks, K. Mackay, R. H. Friend, P. L. Burn, and A. B. Holmes, *Nature*, **347**, 539 (1990).
(2) H. Becker, H. Spreitzer, E. Kruge, H. Schenk, I. Parker, and Y. Cao, *Adv. Mater.,* **12**, 42 (2000).
(3) S. H. Jin, D. S. Koo, C. K. Hwang, J. Y. Do, Y. I. Kim, Y. S. Gal, J. W. Lee, and J. T. Hwang, *Macromol. Res.*, **13**, 114 (2005).
(4) D. M. Welsh, L. J. Kloeppner, L. Madrigal, M. R. Pinto, B. C. Thompson, K. S. Schanze, K. A. Abboud, D. Powell, and J. R. Reynolds, *Macromolecules*, **35**, 6517 (2002).
(5) W. L. Yu, J. Pei, W. Huang, and A. J. Heeger, *Adv. Mater*., **12**, 828 (2000).
(6) Y. H. Kim, J. C. Park, H. J. Kang, H. S. Kim, J. H. Kim, and S. K. Kwon, *Macromol. Res.*, **13**, 403 (2005).
(7) X. Gong, P. K. Iyer, D. Moses, G. C. Bazan, A. J. Heeger, and S. S. Xiao, *Adv. Funct. Mater*., **13**, 325 (2003).
(8) F. Steuber, J. Staduigel, M. Stössel, J. Simmerer, A. Winnacker, H. Spreitzer, F. Weissörtel, and J. Salbeck, *Adv. Mater*., **12**, 130 (2000).
(9) H. Yan, P. Lee, N. R. Armstrong, A. Graham, G. A. Evmenenko, P. Dutta, and T. J. Marks, *J. Am. Chem. Soc.*, **127**, 3172 (2005).
(10) M. Ree, *Macromol. Res.*, **14**, 1 (2006).
(11) Y. Choe, S. Y. Park, D. W. Park, and W. Kim, *Macromol. Res*., **14**, 38 (2006).
(12) W. S. Shin, S. C. Kim, E. J. Lee, S. M. Park, S. H. Jin, J. W. Lee, and Y. S. Gal, *Mol. Cryst. Liq. Cryst*., **471**, 335 (2007).
(13) C. D. Muller, A. Falcou, and N. Reckefuss, *Nature*, **421**, 829 (2003).
(14) K. L. Chan, M. J. McKiernan, C. R. Towns, and A. B. Holmes, *J. Am. Chem. Soc.,* **127**, 7662 (2005).